Korean J. Chem. Eng., 36(2), 305-311 (2019)
DOI: 10.1007/s11814-018-0195-5

pISSN: 0256-1115
eISSN: 1975-7220

Effect of substrate off-orientation on the characteristics of GaInP/AlGaInP single heterojunction solar cells

Junghwan Kim*,† and Hyun-Beom Shin**

*Department of Energy and Mineral Resources Engineering, Sejong University, Seoul 05006, Korea
**Korea Advanced Nano Fabrication Center, Suwon, Gyeonggi-do 16229, Korea
(*Received 6 September 2018 • accepted 17 November 2018*)

Abstract−The effects of GaAs substrate off-orientation on GaInP/AlGaInP heterojunction solar cells were investigated. The performances of solar cells fabricated on 2° and 10° off GaAs substrates were compared. The short circuit current densities were 10.44 mA/cm^2 for the 10° off sample, 7.15 mA/cm^2 and 7.41 mA/cm^2 for the 2° off samples, which showed 30% higher short-circuit current density for 10° off samples. Also, 30% higher external quantum efficiencies and smooth surface morphology were observed in the solar cell fabricated on the 10° off GaAs substrate. Secondary ion mass spectrometry depth profiles showed that the solar cells on 2° off substrates had a 20-times higher oxygen concentration than the solar cells on 10° off GaAs substrate in the n-GaAs/GaAs buffer layer. The 30% reduction for the solar cells on 2° substrates in short circuit current density (J_{sc}) was attributed to the higher oxygen concentration of the 2° off samples than the 10° off samples. I-V characteristics comparison between different front contact grid patterns was also performed for optimization of grid contacts. A 0.47 V bandgap-voltage offset, one of the device performance figures of merit to compare PV cells with different materials, was obtained.

Keywords: Heterojunction Solar Cell, Substrate Off-orientation, Impurity Incorporation, GaInP/AlGaInP

INTRODUCTION

GaAs substrate off-orientation has an effect on the quality of epitaxial layers grown on the substrate such as bandgap energy, doping characteristics, surface morphology and impurity incorporation [1-4]. These properties, which depend on substrate off-orientation angle, are major factors that determine the performance of solar cells. To achieve high performance of PV cells, it is critical to obtain high quality epitaxially grown III-V compound semiconductor materials. Consequently, it is essential to understand how the off-orientation angles of GaAs substrates affect the quality of epitaxial layers on these substrates and the performance of PV cells. GaInP and AlGaInP have been used in III-V compound semiconductor photovoltaic (PV) cells. GaInP is used for the top cell in multijunction (MJ) PV cells, which have achieved the highest current conversion efficiency [5]. In conventional PV cells that use a pn homojunction in single-junction PV cells or in each sub cell of MJ PV cells, electron-hole pairs are generated in the depleted pn homojunction and the photogenerated electrons and holes transport to opposite electrodes through the depletion region. Since the carrier transit velocity of holes is slower than that of electrons, the probability of carrier recombination increases if electrons and holes are generated while photogenerated carriers traverse the same depleted region. This recombination in the depletion region is called a Sah-Noyce-Shockley recombination [6]. Under high intensity illumination conditions such as a concentrated PV system, this recombination in the depletion and transition layer can have a more significant effect on the current-voltage characteristics of PV cells because the increased photogenerated electron-hole pairs result in increased space-charge screening. The screening effect causes lower built-in potential, which in turn slows the carrier transport and thus increases carrier recombination. A heterojunction structure has been used in silicon-based PV cells and organic PV cells. In silicon-based PV cells, heterojunction with an intrinsic thin layer (HIT) structure has shown the highest current conversion efficiency by reducing recombination loss [7]. For organic solar cells, bulk heterojunction structures were employed to improve poor charge separation and charge transport of organic materials [8-12]. In III-V semiconductor materials, heterojunction PV cells can have advantages in achieving high efficiency that are related to reduced carrier recombination loss, increased open circuit voltage and lower series resistance [13]. GaInP has been the most widely used material for top cells and AlGaInP has been used for window layers in MJ PV cells. However, single heterojunction PV cells composed of GaInP/AlGaInP have hardly received attention, and the possibility of efficiency improvement has not been explored extensively for applications with top cell multijunction PV cells. Even though heterojunction structure has an advantage for achieving higher open circuit voltage, and reducing carrier recombination loss, high efficiency is not guaranteed because carrier collection efficiency can worsen if impurity states exist in the epilayers. The impurity states are closely related to growth condition such as substrate off-orientation and growth temperature; it is necessary to investigate how the substrate off-orientation influences the performance of solar cells to achieve high efficiency. This paper presents a comprehensive study of the effect of the substrate off-orientation on the performance of solar cells.

†To whom correspondence should be addressed.
E-mail: junghwan@sejong.ac.kr

In this work, p-GaInP/N-AlGaInP single heterojunction solar cell structures were proposed and grown on 2° and 10° off-oriented GaAs substrates using metalorganic vapor phase epitaxy (MOCVD). Epitaxial layers were designed to be lattice-matched to GaAs substrates. Both material characteristics and the performance of solar cells fabricated on these epitaxially grown materials were compared. Significant differences in short circuit current density (J_{sc}) and external quantum efficiencies (EQEs) were observed between solar cells on different offcut angle GaAs substrates. A secondary ion mass spectrometry (SIMS) depth profile was used to investigate the substrate off-orientation angle dependence on the oxygen impurity incorporation in the solar cell epitaxial layers. The significant difference in J_{sc} between solar cells on 2° and 10° off-oriented GaAs substrates was explained by O incorporation.

In the GaInP/GaInAlP single heterojunction solar cell structure, the smaller bandgap GaInP was placed on the front side of the solar cell as an emitter layer and the larger bandgap AlGaInP was used as a base layer. By placing the smaller bandgap GaInP material on top, the light spectrum above the GaInP bandgap is absorbed at the emitter layer and little or no light absorption occurs in the N-AlGaInP layer. Only the electrons generated in the p-GaInP layer transit through the N-AlGaInP layer where there are few or no photogenerated e-h pairs. Therefore, it is possible to reduce the recombination of photogenerated electrons and thus increase current conversion efficiency. Although GaInP has been the most widely used material for top cells and AlGaInP has been used for window layers in MJ PV cells, GaInP/AlGaInP single heterojunction PV cells have not been studied. Recently, it was reported that a single-junction cell with an n-GaInP/P-AlGaInP structure exhibited very high conversion efficiency [14]. Masuda et al. compared the effect of substrate offcut angle on GaInP and AlGaInP single homojunction PV cell performance and reported that no noticeable difference in J_{sc} was observed [15]. We observed a significant difference in J_{sc} and surface morphology between GaInP/AlGaInP single heterojunction PV cells fabricated on two different offcut angle substrates.

EXPERIMENT

1. Cell Structure

The p-GaInP/N-AlGaInP single heterojunction solar cell structures were grown on 2° and 10° offcut n-GaAs substrates by metalorganic vapor phase epitaxy (MOCVD) in the Korea Advanced Nanofabrication Center. The n-GaAs substrates were cut 2° and 10° off the (100) plane toward the <111>A direction. The epitaxial layer structure of heterojunction PV cells consisted of a 200 nm *n*-GaAs contact layer, a 30 nm N-InAlP back surface field (BSF) layer, an 800 nm *N*-AlGaInP (E_g=2.2 eV) base layer, and a 600 nm *p*-GaInP (E_g=1.85 eV) emitter layer followed by a *p*-AlInP window layer (E_g= 2.36 eV), and a *p*-GaAs contact layer on top. All epilayers were lattice-matched to GaAs. The epitaxial layer structures shown in Fig. 1(a) were grown on 2° and 10° off-oriented n-GaAs substrates, which will be called a 2° off 200 nm contact layer and 10° off 200 nm contact layer, respectively. The other structure shown in Fig. 1(b) is basically the same except that the p-GaAs contact layer thickness was reduced to 100 nm and the doping level of the p-GaAs contact layer

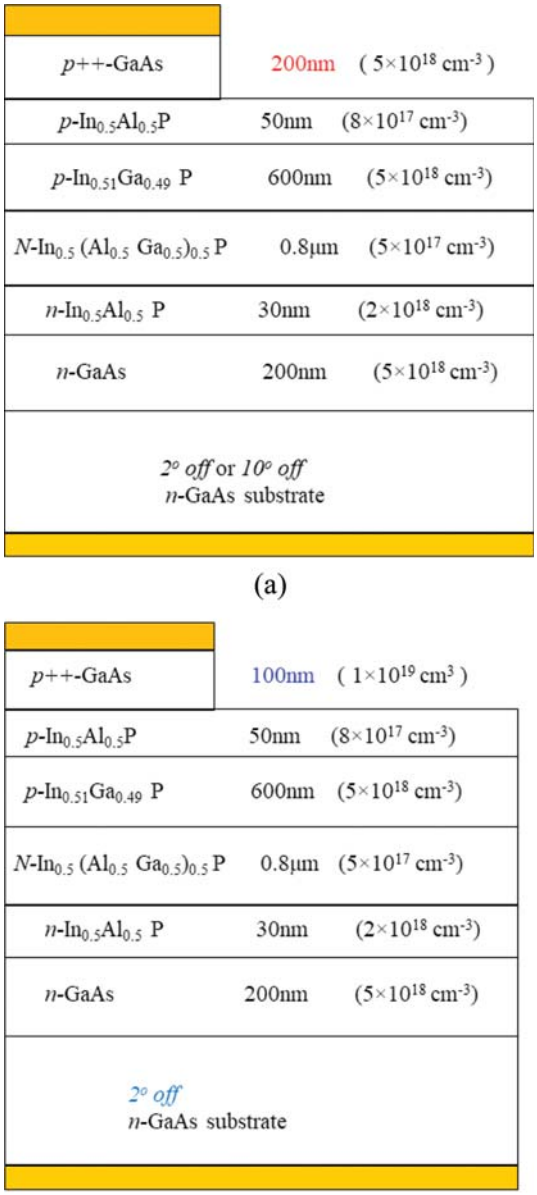

Fig. 1. Epitaxial layer structures of (a) 2° or 10° off with 200 nm GaAs contact layer (b) 2° off with 100 nm GaAs contact layer.

increased to 1×10^{19} cm^3, which will be called a 2° off 100 nm contact layer hereafter. Taking into account that the absorption coefficient of GaInP at 2.2 eV is $\alpha=4\times10^4$ cm^{-1} [16] and the 600-nm-thick p-GaInP layer was used in our epilayer structure, it was estimated that 10% of incident light with energy above 2.2 eV was able to reach the N-AlGaInP base layer. As mentioned in the introduction, as electrons generated in p-GaInP layer transport across the N-AlGaInP layer to the electrode and only small absorption occurs in the N-AlGaInP layer, the recombination of photogenerated carriers can be reduced, thus improving current conversion efficiency.

2. Fabrication

After a front side protective photoresist (PR) was applied, n-metal contacts of AuGe/Ni/Au (80 nm/80 nm/400 nm thickness) were

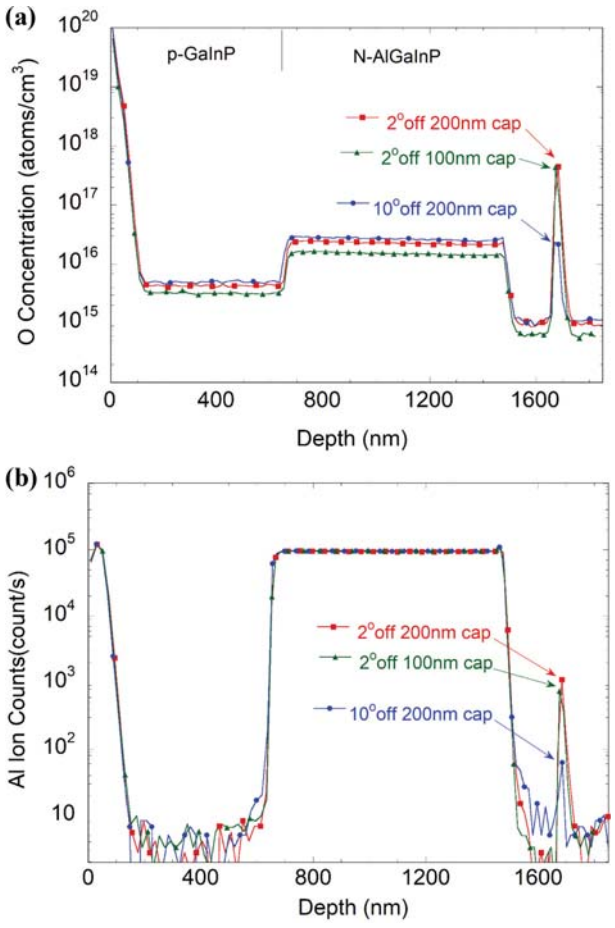

Fig. 2. SIMS depth profiles of (a) oxygen concentration (b) Al content for solar cells on different off-orientation GaAs substrates.

deposited on the back side of a GaAs substrate. For the front side p-metallization, grid patterns were formed by standard photolithography. Ti/Pt/Au were deposited and lifted off. The thicknesses of the p-metals are 20 nm/20 nm/460 nm, respectively. Finally, the p-GaAs contact layer was etched to avoid unintended light absorption at the top contact layer.

RESULTS AND DISCUSSION

1. Secondary Ion Mass Spectrometry Analysis

Fig. 2 shows the SIMS depth profiles of the solar cells fabricated on different off-orientation GaAs substrates. Oxygen is known to be a nonradiative recombination center for GaAs and AlGaAs [17], and for AlGaInP [18]. It has been reported that the oxygen incorporation of a GaAs/AlGaAs heterostructure grown on a GaAs substrate decreased as the GaAs substrate offcut angle increased because of fewer exposed anisotropic sites during epilayer growth [3,17]. It was also observed that oxygen incorporation in the p-GaInP layer grown by molecular beam epitaxy formed deep levels [19]. When oxygen-related levels act as traps, the photogenerated electrons and holes can be captured in these intermediate energy levels caused by the oxygen-related defects. The captured electrons and holes recombined and were not able to convert into current. We found that both aluminum (Al) content and oxygen (O) concentration followed the same trend and showed distinct differences only in the n-GaAs/GaAs buffer layer, which are around a depth of 1,680 nm, between the 2° off substrate and 10° off substrate sample. Other than the n-GaAs/GaAs buffer layer, O concentration does not depend on substrate off-orientation angles. Some research groups have reported the off-orientation dependence of impurity incorporation in AlGaAs/GaAs [20] and in AlGaInP [2], and others have reported the contrary [15]. Our results about O impurity incorporation dependence are different from these previous reports because only the AlGaP BSF layer indicated a substrate offcut angle dependence. Other elements such as indium (In), phosphide (P), gallium (Ga), and arsenide (As) are independent of substrate off-orientation. The O concentration indicated a 20-times difference between the 2° off substrates and 10° off substrate in the n-GaAs/GaAs buffer layer, as seen in Fig. 2(a). The O concentrations are 4.4×10^{17} atom/cm^3 for both solar cells on 2° off substrates, and 2.2×10^{16} atom/cm^3 for the solar cell on the 10° off substrate. The Al content of the 2° off sample samples is more than 12-times higher than the 10° off substrate sample in the n-GaAs/GaAs buffer layer. Al ion counts in Fig. 2(b) are 1,107 count/sec for 2° off with a 200 nm contact layer sample, 744 count/sec for 2° off with a 100 nm contact layer sample, and 64 count/sec for 10° off with a 200 nm contact layer sample. The variation of oxygen concentration follows the Al content. It has been known that the oxygen concentration decreases as GaAs substrates are misoriented from (100) toward (111)A. We speculate that the O at the depth of 1,680 nm was caused by O atoms from growth ambient. During the growth, when GaAs surface was exposed for a relatively long time at the beginning of the growth process in a growth chamber, O impurity atoms were attached more easily to the surface of the 2° off substrate than the surface of the 10° off substrate, and the attached O atoms actively reacted with Al atoms. Once the growth process was stabilized at higher partial pressures of source materials, then the O incorporation decreased as O atoms were competing with group V materials such as As and P atoms for group V sites [21]. A more systematic investigation is required to understand why the O and Al spike were observed only in the n-GaAs/GaAs buffer layer and it will be a future work.

2. Morphology

The surface morphology of two samples grown on 2° and 10° off GaAs substrates was analyzed using atomic force microscopy (AFM). The $10\times10\ \mu m^2$ AFM scan images of both surfaces are shown in Fig. 3. For the 2° off substrates samples, the values of root mean square (RMS) surface roughness are 3.10 nm and 3.45 nm for the 200 nm contact layer sample and the 100 nm contact layer sample, respectively. For the 10° off sample, the RMS roughness value is 1.13 nm. Our AFM results showed that the 10° off sample has a smoother surface than the two 2° off samples. According to the SIMS profile results in the previous section, the O concentration of the 10° off substrate is much lower than the two 2° off substrate samples. We can conclude that high O concentration results in increasing surface roughness. Other researchers reported that the surface became smoother as the GaAs substrate off-orientation angle increased due to less oxygen incorporation and higher oxygen impurities were observed in rougher surfaces in GaAs/AlGaAs

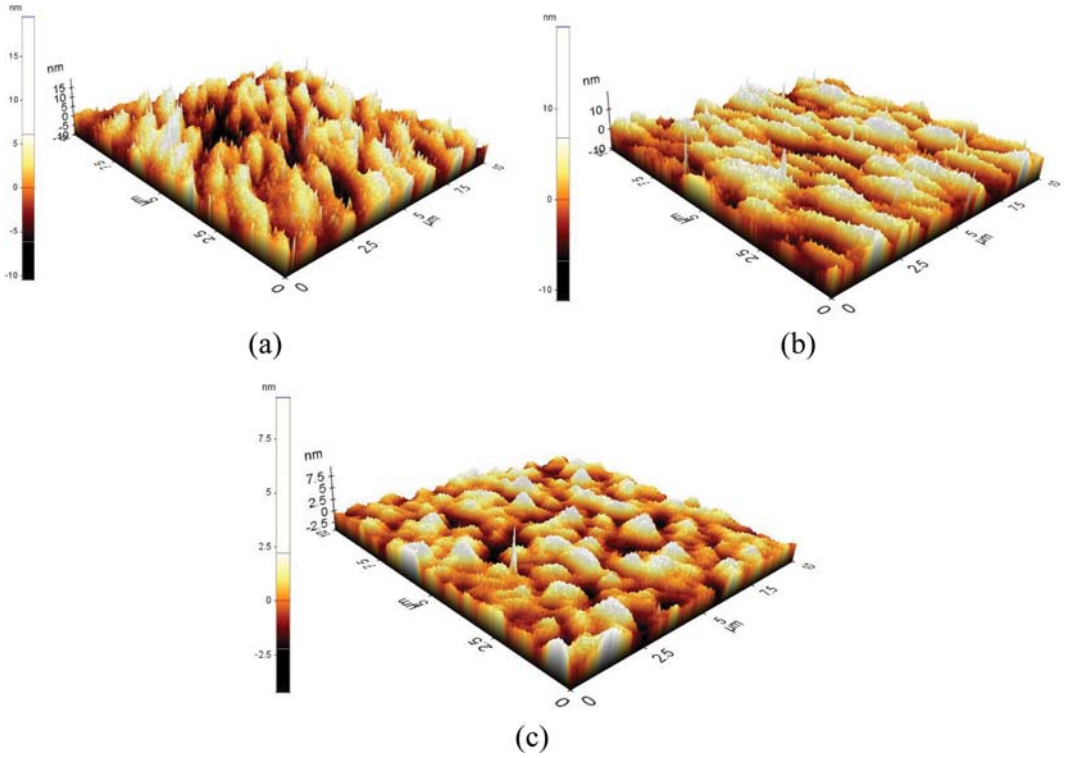

Fig. 3. AFM scan images of 10×10 μm^2 (a) surface of 2° off 200 nm GaAs contact layer (b) 2° off 100 nm GaAs contact layer (c) 10° off 200 nm GaAs contact layer.

structures using secondary ion mass spectrometry (SIMS) profile analysis [20].

3. Thickness of Epitaxial Layers

The thicknesses of grown epitaxial layers were measured using scanning electron microscopy (SEM) to see whether the epilayer thicknesses were grown as designed. The cross sections of three samples are shown in Fig. 4. It has been known for Cu-Pt type ordering in GaInP and GaAlInP materials grown by MOCVD [22]. This ordering depends on growth conditions such as growth temperature and III/V ratio [23] and can affect the bandgaps of the grown epilayers, which are closely related to the electrical and optical properties of solar cells. The *p*-GaInP absorption layer thicknesses, where major absorption occurs, were 538 nm for the 2° off 200 nm contact layer, 565 nm for the 2° off 100 nm contact layer and 543 nm for the 10° off 200 nm contact layer samples, respectively, and the thicknesses of other epilayers were similar. The thick-

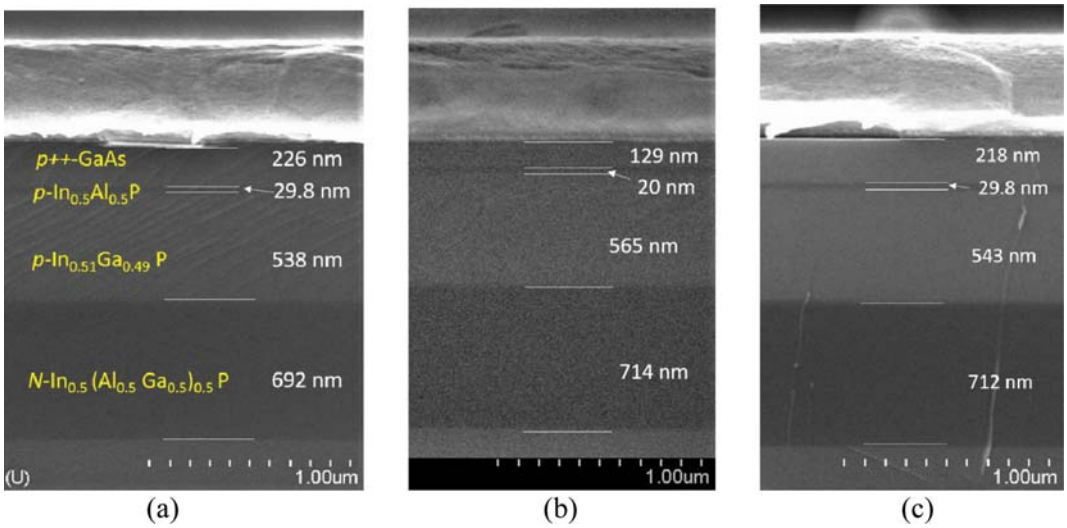

Fig. 4. SEM images of cross-sections of GaInP/GaAlInP single heterostructures grown on GaAs substrates (a) 2° off with 200 nm contact layer (b) 2° off with 100 nm contact layer (c) 10° off 200 nm contact layer.

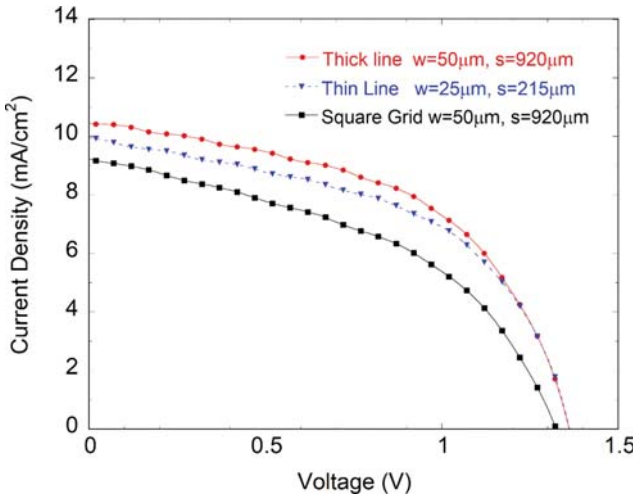

Fig. 5. Current-voltage comparison between different grid patterns for 5 mm×5 mm PV cells.

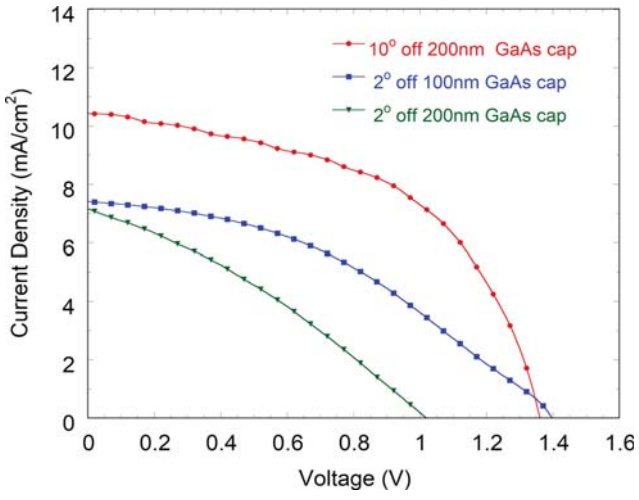

Fig. 6. Current density-voltage measurement results for 5 mm×5 mm PV cells with grid contact of 50 μm width and 920 μm spacing fabricated on 2° and 10° off-cut GaAs substrates under 1-sun condition.

ness of GaInP and GaAlInP layers was slightly thinner than designed but almost identical in all three samples.

4. Comparison of I-V Characteristics Between Different Grid Patterns

The conversion efficiency of PV cells is closely related to metal contact grid patterns. The major losses related to metal grid patterns are shadowing effect, emitter layer resistance, and grid metal resistance. The current density-voltage (J-V) characteristics measured from 5 mm×5 mm area solar cells on a 10° off substrate were compared between PV cells with different contact patterns, and the results are shown in Fig. 5. The solar cells were measured under a 1-sun illumination condition without anti-reflection coating (ARC). Three different types of p-contact electrodes were used in the I-V characteristics comparison. The first one is a square grid pattern with 50 μm width and 920 μm spacing electrode lines crossing each other (square grid); the second is a line grid pattern with 50 μm width line electrodes with 920 μm spacing (thick line grid); and the third one is a line grid pattern with 25 μm width line electrodes with 215 μm spacing (thin line grid). The measured short circuit current densities (J_{sc}) are 9.23 mA/cm^2 for the square grid, 9.96 mA/cm^2 for the thin line grid, and 10.44 mA/cm^2 for the thick line grid. The open circuit voltages (V_{oc}) are 1.32 V for the square grid cell and 1.36 V for both thin line and thick line grid cells. The grid with 50 μm width and 920 μm spacing line grid showed the best efficiency. The shadow effects due to metal grids were calculated to be 15% shadowing for the square grid, 12% for the thick line grid and 18% for the thin line grid, respectively. The thin line grid solar cell showed higher short circuit current density (J_{sc}) than the square grid cell, though the shadow effect in the thin grid cell was larger. This indicates that the widths and spacings of grid lines can be further optimized.

5. I-V Characteristics Analysis Between Different Off-orientation Angle Substrates

The current density-voltage (J-V) characteristics of PV cells under a 1-sun illumination condition are shown in Fig. 6. Three types of solar cells on a 2° off substrate with a 200 nm contact layer, 2° off substrate with a 100 nm contact layer and 10° off substrate with a 200 nm contact layer were compared. The measurement results were obtained from 5 mm×5 mm area devices with 50 μm width and 920 μm spacing line grids (thick line grid), which showed the best efficiency, as shown in the previous section. The short circuit current densities (J_{sc}) were 7.15 mA/cm^2 for the 2° off substrate with a 200 nm contact layer, 7.41 mA/cm^2 for the 2° off substrate with a 100 nm contact layer and 10.44 mA/cm^2 for the 10° off substrate with a 200 nm contact layer. The solar cell on the 10° off substrate showed approximately 30% higher J_{sc} than the other two solar cells on 2° off substrates. Both the J_{sc} of the solar cells on 2° off substrates looked pinned at a similar value. The open circuit voltages were 1.02 V for the 2° off substrate with a 200 nm contact layer, 1.40 V for the 2° off substrate with a 100 nm contact layer, and 1.36 V for the 10° off substrate with a 200 nm contact layer. In J-V curve, the solar cell on the 10° off substrate exhibited higher shunt resistance than both solar cells on 2° off substrates. As these two results combined, the 10° off samples had higher fill factors and thus achieved better efficiency.

In SIMS depth profile analysis, the 2° off sample had more oxygen impurity compared to the 10° off sample in the n-GaAs/GaAs buffer layer. We speculate that the higher J_{sc} in the solar cell on the 10° off substrate is attributed to having less oxygen impurity, which is known to be a nonradiative recombination center, in the n-GaAs/GaAs buffer layer than in the other two solar cells on 2° off substrates. Less oxygen impurity means that there are fewer oxygen-related traps in the BSF layer of the solar cell on a 10° off substrate. The 30% difference in J_{sc} between solar cells on 2° offcut substrates and solar cells on 10° offcut substrates could not be due to absorption layer thickness, because the thickness of both p-GaInP and N-GaAlInP in all three epitaxial layers was almost identical as seen in Fig. 4 (SEM thickness measurements). The J-V results suggest that the 10° off GaAs substrate reduces oxygen incorporation in n-GaAs/GaAs buffer layer during epitaxial layer growth and a smaller number of oxygen-related levels results in higher J_{sc}. We conclude that the 30% reduction in J_{sc} for 2° off substrates samples is caused

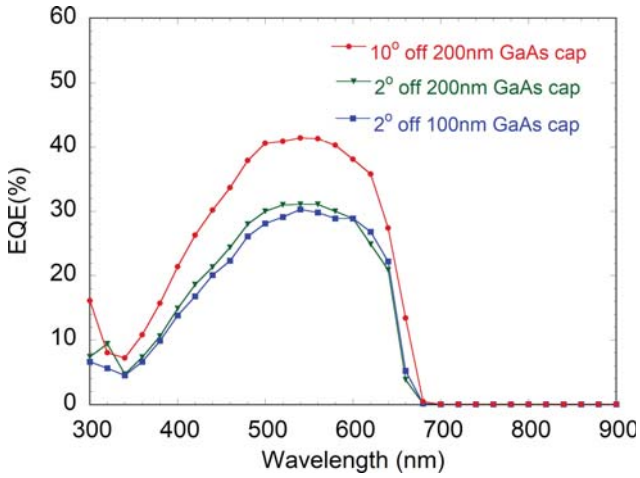

Fig. 7. Comparison of EQE for 5 mm×5 mm PV cells with square grid contact with 50 μm width and 920 μm spacing.

by the 20-times higher O concentration in N-GaAs/GaAs buffer layer. Lower efficiency caused by oxygen vacancy level was also reported in the organic solar cell [24]. It can be seen from the J-V characteristics that a solar cell with a thin contact layer (100 nm) and a high doping level (1×10^{19} cm^{-3}) show better V_{oc} and thus have better efficiency. The efficiency of the 10° off sample is 7.4% with the fill factor (FF) of 0.52. If the solar cells were measured with ARC, then J_{sc} will be increased about 1.5-times because 30% of light is reflected at the surface of solar cells. The low fill factor also needs to be improved by optimizing epitaxial layers. Assuming 80% of FF with improved shunt resistance and ARC, then the efficiency is expected to improve at least to 16% for V_{oc}=1.36 V, J_{sc}=14.9 mA/cm^2. This suggests that there is still room for further optimization, such as the thickness of the GaInP layer and doping levels, to improve efficiency.

6. External Quantum Efficiency

To obtain the spectral absorption response of fabricated PV cells, external quantum efficiency (EQE) was measured, and the results are shown in Fig. 6. The EQE of the cell on the 10° off sample shows a 38% higher response for wavelengths shorter than 680 nm, which corresponds to the GaInP bandgap (1.85 eV). The EQE results agreed well with the J_{sc} result, which was about 30% higher for the solar cell on 10° off with a 200 nm contact layer. The maximum EQE reached 41% for the solar cell on the 10° off substrate, 31% for the cell on the 2° off with a 200 nm contact layer, and 30% for the cell on 2° off with a 100 nm contact layer at 540 nm, respectively. The 41% EQE seems to be low, but we note that our EQE data were measured without an anti-reflection coating and 12% of light was blocked by a shadow effect due to metal contacts. When these losses due to reflection and shadowing, which amount to a 40% loss of incident light, are considered, the internal quantum efficiency (IQE) is estimated to be approximately 67%. Since our PV cells have a relatively thin 600-nm-thick p-GaInP absorption layer, the 67% IQE can be further improved when the p-GaInP layer thickness is increased.

The bandgap-voltage offset, $W_{oc}=E_g/q-V_{oc}$, where q is an elementary charge, is one of the device performance figures of merit in order to compare PV cells with different materials. The W_{oc} is a measurement that indicates how large V_{oc} can be obtained at a given E_g. PV cells with different materials have a wide range of energy bandgaps, and thus varying V_{oc}. It is considered that the smaller W_{oc} is, the better the quality of PV cells is. In our single heterojunction PV cell in this report, an E_g of 1.84 eV obtained from EQE and V_{oc} of 1.37 V from IV measurement gives a W_{oc} of 0.47 V.

CONCLUSION

We have proposed and fabricated single heterojunction p-GaInP/N-AlGaInP PV cells for applications for top cells in MJ PV cells. For high quality epitaxially grown materials to achieve high efficiency, we investigated the effect of substrate off-orientation angle on the performance of GaInP/AlGaInP heterojunction PV cells. Solar cells were fabricated on 2° and 10° off-oriented GaAs substrates and the current density-voltage characteristics, EQE and their surface morphology were compared. The PV cells on 10° off GaAs substrates showed 30% higher J_{sc} and EQE than the PV cells on 2° off substrates. From a SIMS depth profile, the higher J_{sc} of 10° off cells was attributed to less oxygen incorporation in the n-GaAs/GaAs buffer layer during epitaxial layer growth. We found that 20-times higher O incorporation in one epitaxial layer on 2° off substrates than on 10° off substrate caused 30% reduction in J_{sc}. A W_{oc} of 0.47 V was achieved. Although further optimization of epilayer design such as layer thicknesses and doping levels is required for higher conversion efficiency, we have demonstrated the feasibility of a single heterojunction p-GaInP/N-AlGaInP PV cell.

ACKNOWLEDGEMENT

This research was supported by the Nano-Material Technology Development Program through the National Research Foundation of Korea (NRF) funded by the Ministry of Science, ICT and Future Planning (2009-0082580).

REFERENCES

1. M. Suzuki, Y. Nishikawa, M. Ishikawa and Y. Kokubun, *J. Cryst. Growth*, **113**, 127 (1991).
2. M. Kondo, C. Anayama, N. Okada, H. Sekiguchi, K. Domen and T. Tanahashi, *J. Appl. Phys.*, **76**, 914 (1994).
3. D. C. Radulescu, G. W. Wicks, W. J. Schaff, A. R. Calawa and L. F. Eastman, *J. Appl. Phys.*, **63**, 5115 (1988).
4. T. Suzuki, A. Gomyo and S. Iijima, *J. Cryst. Growth*, **99**, 60 (1990).
5. R. M. France, J. F. Geisz, I. Garcia, M. A. Steiner, W. E. McMahon, D. J. Friedman, T. E. Moriarty, C. Osterwald, J. Scott Ward, A. Duda, M. Young and W. J. Olavarria, *IEEE J. Photovoltaics*, **5**, 432 (2015).
6. C. T. Sah, R. N. Noyce and W. Shockley, *Proceedings of the IRE*, **45**, 1228 (1957).
7. K. Masuko, M. Shigematsu, T. Hashiguchi, D. Fujishima, M. Kai, N. Yoshimura, T. Yamaguchi, Y. Ichihashi, T. Mishima, N. Matsubara, T. Yamanishi, T. Takahama, M. Taguchi, E. Maruyama and S. Okamoto, *IEEE J. Photovoltaics*, **4**, 1433 (2014).
8. B. Zhang, D. H. Lee, H. Chae, C. Park and S. M. Cho, *Korean J.*

Chem Eng., **27**, 999 (2010).
9. H. Kim, S. Nam, J. Jeong, S. Lee, J. Seo, H. Han and Y. Kim, *Korean J. Chem Eng.*, **31**, 1095 (2014).
10. H. H. Cho, C. H. Cho, H. Kang, H. Yu, J. H. Oh and B. J. Kim, *Korean J. Chem Eng.*, **32**, 261 (2014).
11. I. H. Yoo, S. S. Kalanur, K. Eom, B. Ahn, I. S. Cho, H. K. Yu, H. Jeon and H. Seo, *Korean J. Chem Eng.*, **34**, 3200 (2017).
12. V. H. T. Pham, N. T. N. Truong, T. K. Trinh, S. H. Lee and C. Park, *Korean J. Chem Eng.*, **33**, 678 (2016).
13. D. L. Feucht, *J. Vac. Sci. Technol.*, **14**, 57 (1977).
14. J. F. Geisz, M. A. Steiner, I. García, S. R. Kurtz and D. J. Friedman, *Appl. Phys. Lett.*, **103**, 041118 (2013).
15. T. Masuda, S. Tomasulo, J. R. Lang and M. L. Lee, *J. Appl. Phys.*, **117**, 094504 (2015).
16. M. Moser, C. Geng, E. Lach, I. Queisser, F. Scholz, H. Schweizer and A. Dörnen, *J. Cryst. Growth*, **124**, 333 (1992).
17. N. Chand, A. S. Jordan and S. N. G. Chu, *Appl. Phys. Lett.*, **59**, 3270 (1991).
18. M. Kondo, N. Okada, K. Domen, K. Sugiura, C. Anayama and T. Tanahashi, *J. Electron. Mater.*, **23**, 355 (1994).
19. N. Xiang, A. Tukiainen and M. Pessa, *J. Electron. Mater.*, **13**, 549 (2002).
20. H. W. Yu, E. Y. Chang, H. Q. Nguyen, J. T. Chang, C. C. Chung, C. I. Kuo, Y. Y. Wong and W. C. Wang, *Appl. Phys. Lett.*, **97**, 2008 (2010).
21. M. Hata, H. Takata, T. Yako, N. Fukuhara, T. Maeda and Y. Uemura, *J. Cryst. Growth*, **124**, 427 (1992).
22. B. A. Philips, A. G. Norman, T. Y. Seong, S. Mahajan, G. R. Booker, M. Skowronski, J. P. Harbison and V. G. Keramidas, *J. Cryst. Growth*, **140**, 249 (1994).
23. A. Gomyo, T. Suzuki and S. Iijima, *Phys. Rev. Lett.*, **60**, 2645 (1988).
24. M. Zafar, J.-Y. Yun and D.-H. Kim, *Korean J. Chem Eng.*, **34**, 1504 (2017).